RESPONSE OF OPEN CHANNEL FLOW TO A SUDDEN CHANGE FROM ROUGH TO SMOOTH SURFACE

Franklin N. Krampa-Morlu
Department of Mechanical Engineering,
University of Saskatchewan
57 Campus Drive
Saskatoon, Saskatchewan, S7N5A9, Canada
fnk382@mail.usask.ca

Ram Balachandar
Department of Civil and Environmental Engineering,
University of Windsor
Windsor, Ontario, N9B3P4, Canada
rambala@uwindsor.ca

ABSTRACT

Measurements of mean velocity and higher order turbulence statistics are presented for the study of flow response and relaxation in the presence of a sudden change in surface geometry from rough to smooth surface in an open channel. The rough surface was made up of spherical ribs. The ribs were constructed using spherical glass beads of diameter D (or k) = 12.5 mm joined together transversely across the width of the channel. Two types of roughness, a d-type and an intermediate-type, having pitch to height ratio of 2 and 4, respectively, were used in the study. For the rough wall data obtained on the crest of the rib, the intermediate-types indicated a higher roughness effect. After the sudden change, mean velocity profiles relax rapidly to a smooth wall type profile in the near wall region. After the sudden change in roughness, the mean velocity rapidly assumed a smooth-wall-like behaviour in the near wall region. The relaxation to the smooth-wall behaviour was rather slow for the higher order turbulence statistics near the wall. In the outer region, the mean and turbulence quantities showed that the flow is still relaxing toward a smooth wall type flow.

INTRODUCTION

Many engineering flow applications occur on surfaces with either naturally or artificially varying roughness. As well, there are many flows where sudden changes in surface roughness are encountered (Tani, 1987). For example, the flow encountered on in-service turbine blades, atmospheric boundary layers occurring over rough and smooth surfaces such as the land-sea interface (Taylor et al. 1993), and many other engineering and environmental flows. In open channel flows, such as river flows, the surface roughness can vary dramatically. The practical implications of flows in systems of varying geometry of surface roughness have initiated a number of studies to improve the understanding of the flow physics in such systems.

For flow over transverse ribs, the roughness geometry is often divided into two groups, namely, d-type and k-type (Perry et al. 1969). In quantifying the type for evenly spaced ribs, Tani (1987) proposed a demarcation between the d-type and the k-type as $w/k = 4$, where w is the pitch between the roughness elements (ribs) and k is the height of the roughness elements. The d-type roughness is identified by closely spaced ribs such that $w/k < 4$, while those of the k-type are typified by sparsely spaced ribs with $w/k > 4$.

Several investigations have been performed to study the changes in the flow field due to sudden changes in surface roughness (e.g., Antonia and Luxton, 1971; 1972; Grass et al. 1991; Taylor et al. 1993; Avelino, 2000; and Balachandar and Patel, 2002). Antonia and Luxton (1972) studied the flow over a step change in roughness where the smooth surface followed a k-type ($w/k = 4$) rough surface consisting of 3.175 mm square ribs. The smooth surface was aligned with the crest of the roughness elements. It should be noted that in the work of Antonia and Luxton (1972), $w/k = 4$ is regarded as a k-type roughness as opposed to the demarcation of roughness type proposed by Tani (1987) which is adopted in the present study (cf. Cui et al. 2003). In the study of Taylor et al. (1993), the roughness elements were 1.27 mm diameter hemispheres spaced 2.54 mm (i.e., 2 base diameters) apart in a staggered arrangement. Flow over spheres arranged in rows such that $w/k = 1$ has been investigated in open channels in the context of studying the vortical structures over the roughness elements (Grass et al. 1991). More recently, Balachandar and Patel (2002) studied a developing flow over an array of 12.7 mm spheres for a pitch to height ratio of 1.

Most of the previous studies were performed in the wind tunnel. In contrast to the canonical boundary layer flows often observed in wind tunnel experiments, the velocity profile in open channel flow decreases gradually toward the surface from its maximum value at a wall-normal location denoted by $y_{U_{max}}$ to a slightly lower value at the free surface, $y = h$, where h is the depth of the water. Also, in the presence of surface roughness, recent measurements in open channels have shown that the roughness effect extends to the outer region of the flow (Tachie, 2000). Although numerous studies have been performed on smooth and rough surfaces in open channel flows, the study of flow over a step change in surface roughness is scarce. Given the free surface effect in open channel flows and recent observations (Tachie, 2000) that roughness effect

is felt in the outer region, the response and relaxation of the flow due to the sudden perturbation is worth investigating.

The main objective of the present study is to investigate the flow response and relaxation in an open channel due to a sudden change from a rough surface to a smooth surface. Two rough surfaces (see Figures 1 and 2) made from glass beads joined together to form transverse spherical ribs were used. Specifically, the effects of the step change and the roughness type on measured mean velocity and higher order turbulence statistics (i.e., turbulence intensity, skewness and flatness) downstream of the step are of particular interest. Detailed arrangements of the ribs are discussed below. In the present study, the effect of a d-type ($w/k = 2$) and an intermediate-type ($w/k = 4$) roughness on the flow response and relaxation are investigated. Note that, the term 'intermediate' is used to identify the transition of roughness from the d-type to the k-type and vice versa.

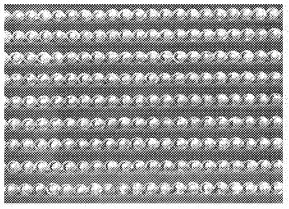

Figure 1: d-type rib roughness, $w/k = 2$.

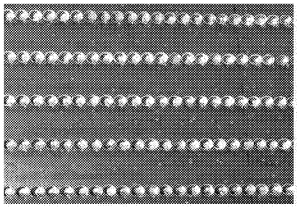

Figure 2: Intermediate-type rib roughness, $w/k = 4$.

Table 1: Summary of test conditions for measurements on the crest of last rib.

Surface Roughness	U_e m/s	δ m	Re_θ	u_τ m/s	Tu %
d-type	0.553	24.1	2000	0.031	3.5
Intermediate-type	0.554	28.0	2500	0.035	3.9

EXPERIMENTAL SET-UP AND PROCEDURE

The Open Channel Flume

The experiments were conducted in a rectangular cross-section open channel flume 0.8 m wide, 0.6 m deep and 10 m long. The sidewalls of the flume were made of transparent tempered glass to facilitate velocity measurements using a laser Doppler anemometer. A contraction and several stilling arrangements used to reduce any large-scale turbulence in the flow preceded the straight section of the channel. The channel bottom was made of brass and the slope, which was adjustable, was ensured to be horizontal for the present study.

Roughness Geometry

In this work, two types of surface roughness, a d-type and an intermediate-type ribs, were used. The ribs were constructed from spherical glass beads of mean height (diameter, D) $k = 12.5$ mm. The beads are attached together and to the channel wall to form transverse ribs that span the entire width of the channel. Sections of the rib arrangements for the two surface types are shown in Figures 1 and 2. Figure 1 shows a section of the rib arrangement of the d-type roughness. Within the test section, 17 spherical ribs were glued to the bottom of the flume for the d-type rib roughness. Figure 2 depicts the corresponding arrangement for the intermediate-type rib roughness, which was made up of 9 ribs over the same distance of the test section as in the case of the d-type roughness.

Measurement Procedure

To enhance and ensure a fully developed turbulent flow, the flow was tripped with a 1.6 mm diameter steel rod. The trip device, positioned 4 m downstream of the contraction and spanning the width of the flume, was glued to the wall of the flume. The depth of flow was 100 mm.

Velocity measurements were carried out along the channel centreline using a one-component fibre-optic laser Doppler anemometer (Dantec Inc.). The present system uses a 300 mW, air-cooled Argon-Ion laser (Ion Laser Technology). The laser Doppler anemometer system is operated in a backscatter mode. Detailed description of the operating parameters of the laser Doppler anemometer used in this study is given elsewhere by Balachandar and Ramachandran (1999) and Krampa-Morlu (2001), among others and therefore avoided here for brevity. The fibre optic probe is mounted on a three-dimensional traversing mechanism. A personal computer (PC) controlled stepper motor drives the traversing mechanism in all three-directions.

Measurements were obtained at axial locations of $x/D =$ 0, 10, 20, and 40. For the present analysis, x is the coordinate axis in the streamwise direction starting from the last rib crest. The flow was found to be two-dimensional with a variation of less than 1.0% of the freestream velocity (i.e., $U_e = 0.995U_{max}$). Close to the bottom wall, sufficient data was taken by traversing the measurement probe in small distances of 0.05 mm. For flow over each roughness surface, the maximum velocity was approximately 0.55 m/s. In the perturbed region downstream of the last rib arrangement (i.e., on the smooth surface), the maximum velocity decreased by about 5% relative to that measured on the crest of the rib over the locations considered. The 5% decrease in the maximum velocity at 10 rib diameters implies a negligible change in the pressure gradient. During the experiment, the change in water surface elevation was less than 1 mm over the test section. A summary of the test conditions for the rough wall data is provided in Table 1. In the table, the local turbulence intensity (Tu) of the flow is specified at $y = \delta$, where the velocity is 99.5% of the maximum velocity; Re_θ denote the Reynolds number based on the momentum thickness (θ), and u_τ is the friction velocity.

Uncertainty estimates were obtained by assuming a 95% confidence interval for Gaussian distributions. Following Schwarz et al. (1999), the error due to the beam-crossing angle, σ_o, was adopted as $\sigma_o = 0.4\%$. The uncertainty of the statistical quantities depends on both the sample size (N) and the root-means-square (rms) level for the mean quantity. Typically, the uncertainties of the mean velocity (U) and the turbulence intensity (u_{rms}) are 0.9% and 1.4%, respectively, close to the crest of the rib. At $x/D = 10$, similar uncertainties were estimated in the near wall region; the corresponding values are 0.5% and 1.1%, respectively, in the overlap ($y^+ \approx 60$) and the outer regions ($y^+ \approx 1000$).

RESULTS AND DISCUSSION

Determination of friction velocity

The friction velocity was determined using three methods. On the rough wall, the Clauser plot technique and the velocity defect formulation (Krogstad et al. 1992) were employed, while on the smooth wall after the step change, the modified fifth order polynomial relation for open channel flows (Tachie 2000), in addition to the two methods mentioned above, was used.

For turbulent rough wall flows, the Clauser plot technique is commonly used to estimate the skin friction and the velocity profile is assumed to follow a logarithmic form, i.e.

$$U^+ = \frac{1}{\kappa}\ln y^+ + B - \Delta U^+, \tag{1}$$

where $U^+ = U/u_\tau$ and $y^+ = yu_\tau/\nu$ are the velocity and wall-normal distance in wall units, respectively; ν is the viscosity; $k = 0.41$ is the von-Kármán constant; $B = 5.0$ is the additive constant for smooth surface; and ΔU^+ is the roughness function for flow over rough surface. The roughness function vanishes for smooth wall flows.

For rough wall flows, the use of the velocity defect law suggested by Krogstad et al. (1992) for the determination of skin friction has attracted significant attention due to the treatment of the wake parameter Π and the estimation of the virtual origin ε. For fully rough flows at low Reynolds number, the log-law (overlap) region becomes narrower, and recent studies indicate that as the roughness function (downward shift of the mean velocity profile) increases, the mean velocity profile becomes concave at the lower part of the wake region. The defect law allows the optimization of Π and refinement of u_τ, as well as the estimation of the virtual origin, ε. In the present work, the fits obtained for both the law of the wall and the defect profiles simultaneously enhanced the accurate determination of both u_τ and Π values for the rough wall data. The form of the defect formulation is given by

$$\frac{U_e - U}{u_\tau} = -\frac{1}{\kappa}\ln\left(\frac{y+\varepsilon}{\delta}\right) + \frac{2\Pi}{\kappa}\left[w(1) - w\left(\frac{y+\varepsilon}{\delta}\right)\right], \tag{2}$$

where

$$w\left(\frac{y+\varepsilon}{\delta}\right) = \frac{1}{2\Pi}\left[(1+6\Pi)\left(\frac{y+\varepsilon}{\delta}\right)^2 - (1+4\Pi)\left(\frac{y+\varepsilon}{\delta}\right)^3\right] \tag{3}$$

is the wake function. For flow over smooth walls, $\varepsilon = 0$. For the rough wall measurements reported herein, the wall normal distance, y, was measured relative to the crest of the roughness elements.

A more reliable approach to determine the friction velocity u_τ for smooth wall flows is to use a fifth order polynomial (George and Castillo, 1997), provided sufficient data points are obtained very close to the wall (typically, for $y^+ = 13$), i.e.,

$$U^+ = y^+ + c_4 y^{+4} + c_5 y^{+5}. \tag{4}$$

From equation (4), the friction velocities were estimated for the smooth wall section using the modified values of the coefficients c_4 and c_5, i.e. $c_4 = -2.7\times10^{-4}$ and $c_5 = 1.33\times10^{-5}$ (Tachie, 2000). Similar to the observations made by Tachie (2000), the data agree with the sub-layer linear relation, $U^+ = y^+$, up to $y^+ = 6$ while the fifth order polynomial profile is in reasonable agreement with the data up to $y^+ = 13$ as shown in Figure 3. The field variables discussed below were scaled using the local wall units, i.e., u_τ as velocity scale and ν/u_τ as the viscous length scale.

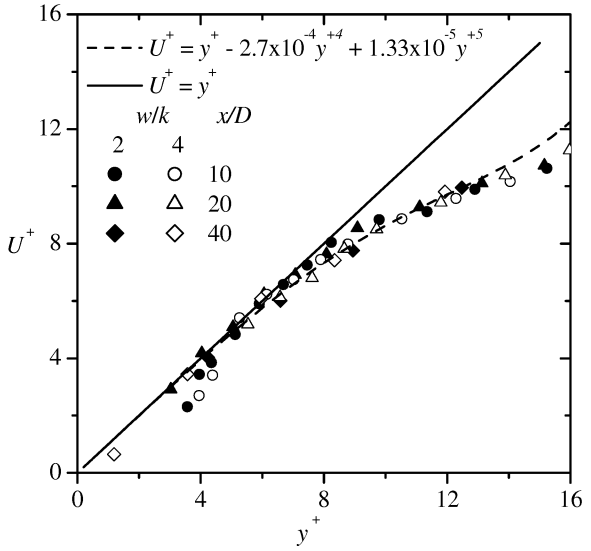

Figure 3: Polynomial fit to the mean velocity in wall units for data on the smooth wall after the sudden change in roughness.

Mean Velocity

Figure 4 shows the mean velocity distributions in wall units for the *d*-type and the intermediate-type rough walls, as well as the smooth surface downstream of the roughness section. The rough wall profiles show a downward shift as expected compared to the traditional smooth wall profile represented by the log-law in this case. The effect of roughness is more pronounced for the intermediate-type roughness than for the *d*-type as is evident by the amount of the downward shift in the figure. A similar trend was observed in the LES simulations by Cui et al. (2003) for flow over square ribs in a channel. However, contrary to the linear overlap region noted in the study of Cui et al. (2003), the profiles on the rough walls reported herein exhibit concave trend.

The response of the mean velocity due to the step change in surface geometry from rough to smooth is demonstrated in the profiles obtained at $x/D = 10$, 20, and 40. The relaxation to a smooth wall flow in the inner region is very rapid for the data obtained for the flow on both roughness types. The rapid relaxation in the near wall region indicates that the flow is locally self preserved and is independent of the type of roughness. Similar observation of near wall flow response was made in the study of Taylor et al. (1993). In the outer region, the flow is remarkably disturbed. However, the tendency of the flow to relax to a traditional smooth wall mean velocity profile is evident with increasing downstream distance. At $x/D = 10$, while the mean velocity in the near wall region is completely relaxed to the linear $U^+ = y^+$ relation, the deviation from the smooth wall form is visible in the overlap region and beyond. The effect of roughness is observed for $y^+ > 30$. At the $x/D = 10$ location, the mean velocity increases abruptly from $y^+ \approx 100$ toward the outer region peaking at $y^+ \approx 1000$.

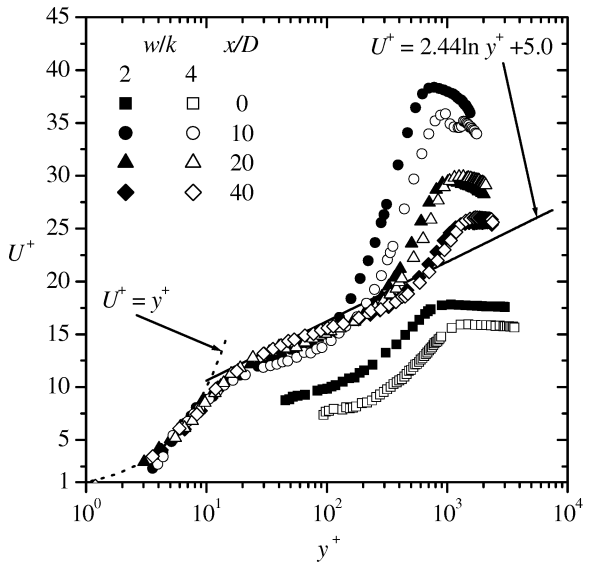

Figure 4: Mean velocity profiles in wall units.

As expected, the effect of the surface roughness on the flow is more pronounce at 10 sphere diameters from the change in roughness (i.e., closest location to the step).

With increasing downstream distance, the overlap region gradually assumes the form of the smooth wall profile. In addition, the slope of the velocity profile in the outer region reduces and the approach to the canonical boundary layer type flow is evident albeit slow compared to the inner region. The data presented here shows that the outer flow is not self preserved compared to the inner flow and, therefore, still relaxing at $x/D = 40$. It can be inferred from the profiles that the wake region is dramatically increased but then tends toward the standard form as the streamwise distance increases. Further downstream, $x/D = 20$ and 40, the roughness effect diminishes, but its presence is still observed in the outer region. The flow over both surfaces produced identical distribution of the mean velocity field. This is expected since after the step, the surface geometry is the same. It is interesting to note that after the step, the flow exhibits roughness effect in the outer region compared to the inner region. As pointed out by Antonia and Luxton (1972), this is indicative of the large proportion of the turbulent energy residing in the large scale turbulence in the outer region rather than in the small scale turbulence in the near wall region.

Streamwise Turbulence Intensity

Figure 5 shows the streamwise turbulence intensity in inner scaling, u^+_{rms}. In Figure 5a, the turbulence intensities for both rib arrangements are constant and flat with a value of $u^+_{rms} \approx 2.3$ in the region $40 < y^+ < 200$, which is a characteristic of recent evidence that roughness effect extends beyond the roughness sub-layer. Overall, the turbulence intensity is slightly higher for the intermediate-type roughness than the *d*-type roughness. Unlike the mean velocity profile, the turbulence intensity is perturbed across the flow depth after the step change from rough to smooth wall as shown in Figures 5b, 5c, and 5d. The effect of the perturbation due to the step change is manifested in increased turbulence intensity toward the outer region. In Figure 5b ($x/D = 10$), the turbulence

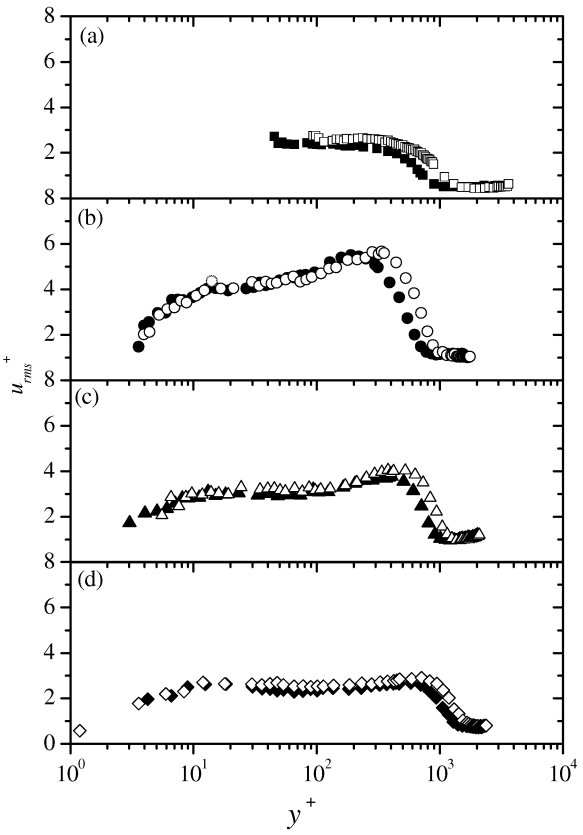

Figure 5: Turbulence intensity profiles in wall units: *the open symbols represent the profiles for the d-type roughness and the solid symbols represent those for the intermediate-type; (a) x/D = 0, (b) x/D = 10, (c) x/D = 20, (d) x/D = 40.*

intensity increases toward the outer region. At $x/D = 10$, the turbulence intensity profiles consist of two peaks occurring at $y^+ \approx 15$ and 300. Note that, the y^+ value for the peak value of the turbulence intensity in the outer region increases with downstream distance. But for $y^+ > 300$, the turbulence intensity did not show any roughness effect. This behaviour is consistent with the other two downstream locations, that is, $x/D = 20$ and 40 as shown in Figures 5c and 5d, respectively. After the step, the profiles of the turbulence intensity decreased rapidly to a minimum at the free surface.

As the downstream distance increases, both the inner and outer regions of the turbulence intensity tend to relax toward the standard smooth wall profile. The decrease in the turbulence intensity from $x/D = 10$ to 20 is much higher than from $x/D = 20$ to 40 signifying a rapid rate of relaxation close to the step. However, it is remarkable to note that at $x/D = 40$, the peak value of the turbulence intensity close to the wall is identical to that of a smooth wall data ($u^+_{rms} = 2.6$) and occurs at $y^+ \approx 12$. Clearly, this suggests that the turbulence intensity is completely relaxed in the inner region at 40 rib diameters from the step, at least for the surface roughness types considered herein. In addition, except for the outer region, the turbulence intensity is identical to that observed for the rough walls at $x/D = 40$ in the overlap region. This can be viewed as the location at which the turbulence intensity of the flow relaxes to the upstream condition on the rough wall.

Higher Order Statistics

Higher order moments such as skewness and flatness are generally used to provide information about the temporal distribution of the velocity fluctuation around its mean value. They can be used to provide some structural information regarding the features of the flow field considered in this work. The skewness and flatness factors are, respectively, defined as

$$S_u = \overline{u^3} / \left(\overline{u^2}\right)^{3/2} \; ; F_u = \overline{u^4} / \left(\overline{u^2}\right)^2, \qquad (5)$$

where u is the streamwise velocity fluctuation. The skewness factor can be used to describe structural information without ambiguity or subjectivity since it retains the sign information. A non-zero skewness factor indicates the degree of temporal asymmetry of the random fluctuation such as acceleration (i.e., sweep) versus deceleration (i.e., ejection) events (Gad-el-Hak and Bandyopadhyay, 1994). On the other hand, a flatness factor larger than 3 is an indication of a peak signal such as the phenomenon of intermittent turbulent events.

Skewness Factor. Figure 6 shows the distributions of skewness factor for flow on both surfaces in wall units. In Figure 6a, the value of the skewness is slightly higher than the corresponding Gaussian probability distribution value of zero for $y^+ < 200$. This suggests that more high-speed fluid weakly dominates the overlap region for the rough surfaces considered herein. Previous studies, (Raupach, 1981) and more recent investigations in open channel flows (Tachie, 2000) have also reported high positive values of skewness for rough wall in the near-wall and overlap regions. This observation is in contrast to that normally observed for smooth wall flows where high positive values of the skewness are confined only in the near-wall region. The dependence of the skewness on the rib arrangement is observed for $y^+ < 200$ and $y^+ > 500$ except close to the free surface of the water. Within the region $200 < y^+ < 500$, the skewness of both surfaces collapse onto each other indicating similar features in the overlap region. The skewness of the intermediate-type roughness attains a minimum value at a higher y^+ (≈ 1000) than that for the d-type roughness, which attains a minimum value at $y^+ \approx 700$.

Focusing attention now to the features of the skewness after the step change, the skewness profiles in Figures 6b, 6c, and 6d slowly assume the characteristics usually exhibited in smooth wall flows with increasing downstream distance. At $x/D = 10$, Figure 6b shows that the skewness for both surfaces are positive in the region $y^+ < 200$, and that for the intermediate-type is higher in the near wall region ($y^+ < 8$). The skewness did not exhibit any roughness effect between $y^+ \approx 8$ and $y^+ \approx 200$, but the positive values of S_u for $y^+ < 200$ indicate that the features of roughness are still present at $x/D = 10$. The positive values of S_u in this region are possibly due to acceleration-dominated events (sweep) from regions away from the wall. In the outer region, the skewness exhibits similar features and roughness effects as observed for the data at $x/D = 0$ (i.e., Figure 6a). But for the level of minimum values of the skewness (which increases) the roughness effect on the skewness in the outer region is consistent even up to $x/D = 40$ (see Figures 6c and 6d). As the downstream distance increases, it can be observed that the positive value of skewness in the buffer and overlap regions decreases and a constant skewness level is observed for the overlap region. In Figure 6d, though the skewness changes sign at approximately $y^+ = 12$, the extent of negative skewness is very narrow

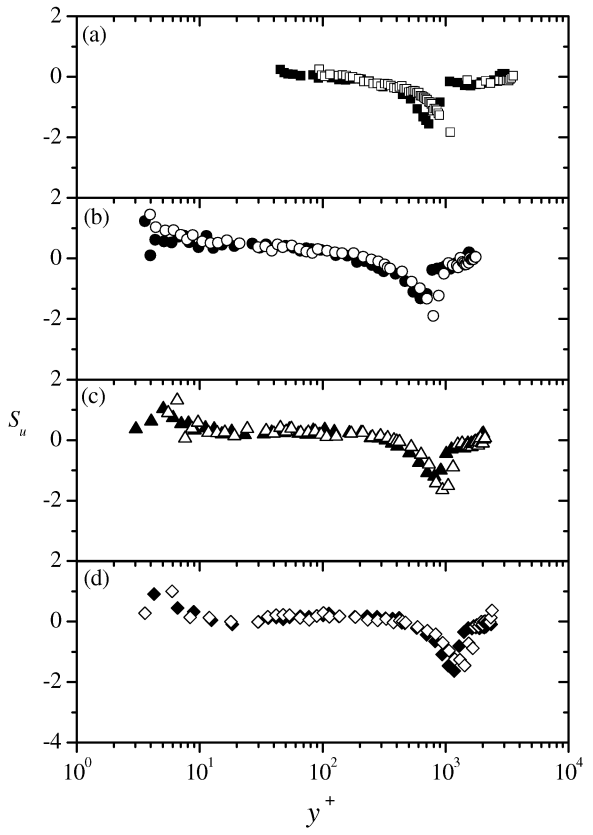

Figure 6: Skewness factor distributions: *Symbols as in Figure 5; (a) $x/D = 0$, (b) $x/D = 10$, (c) $x/D = 20$, (d) $x/D = 40$.*

($17 < y^+ < 30$) suggesting that negative signals occur less frequently. In the overlap region (i.e., for $30 < y^+ < 300$), the flow is likely dominated by low sweep events for the small values of skewness in that region.

Flatness Factor. The flatness profiles are shown in Figures 7a, 7b, 7c, and 7d for both surfaces at $x/D = 0$, 10, 20, and 40, respectively. From these figures, large positive values of F_u are observed in the wall region for data at $x/D = 10$ and 20, and beyond the overlap region for both rib arrangements. In the wall region, the high values of F_u and S_u, indicate that bursting events (sweep and ejection processes) are intermittent in that region. From Figures 6b and 7b, and 6c and 7c, respectively, it is evident that the intermittent bursting events are not influenced by the types of roughness used in the present study. The profiles at $x/D = 40$ show a minimum value in the flatness at approximately $y^+ = 12$. This is the wall-normal location closest to the wall at which the turbulence intensity is maximum (Figure 5d) and the skewness factor changes sign from positive to negative (Figure 6d). This observation indicates that, at least for the near wall region, the higher order moments (up to the flatness factor) in the streamwise direction show the characteristic features of flow over a smooth wall. In the overlap region, the flatness is constant and close to the Guassian value of 3 for all the measurement locations considered. In the outer region, the roughness effect at all streamwise locations is unique such that the flatness deviates and peaks around the location of maximum velocity. This location corresponds to the point at which the value of the

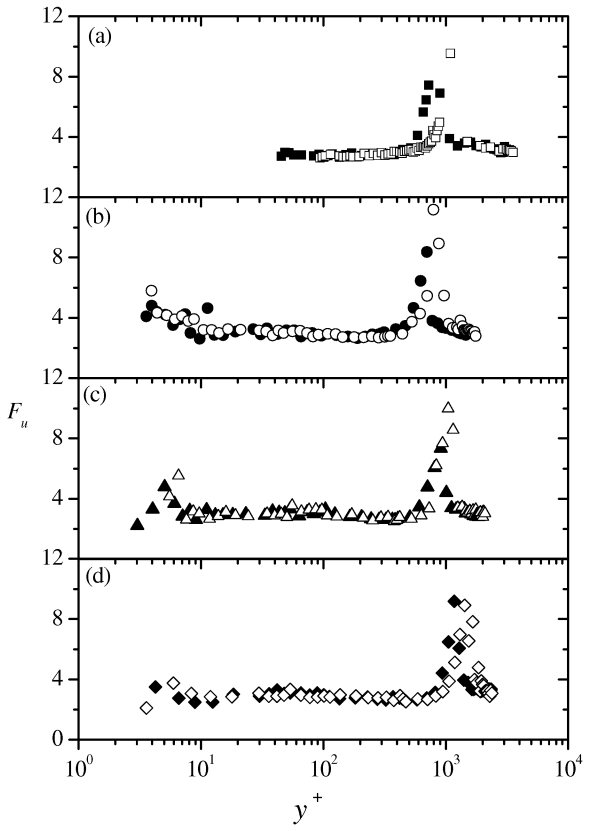

Figure 7: Flatness factor distributions: *Symbols as in Figure 5; (a) x/D = 0, (b) x/D = 10, (c) x/D = 20, (d) x/D = 40.*

skewness is lowest. Note that, the roughness type does not influence the flatness in the free surface region.

CONCLUSIONS

The step change in surface roughness from rough wall, consisting of spherical ribs, to smooth wall in open channel flows has been shown to have significant effect on the mean velocity and streamwise turbulence statistics. The response of the flows was investigated for two types of roughness, namely, a *d*-type and an intermediate-type roughness.

For the rough wall data obtained on the crest of the rib, the intermediate-type indicated a higher roughness effect. After the sudden change, the mean velocity profiles relax rapidly to a smooth wall type profile in the near wall region. The streamwise turbulence intensity, skewness factor, and flatness factor profiles show a rather slow relaxation close to the wall. For the downstream locations considered, the mean and higher order turbulence statistics did not reach a self-preservation state in the outer region. The slow relaxation in the outer region revealed the effect of the two types of rib arrangements used in the study. While the rapid relaxation to a smooth wall flow eliminates any roughness effect in the near wall region, roughness effect is observed in the outer region.

REFERENCES

Antonia, R. A., and Luxton, R. E., 1971, "The response of a turbulent boundary layer to a step change in surface roughness, Part 1: smooth to rough", *Journal of Fluid Mechanics*, Vol. 48, 721-761.

Antonia, R. A., and Luxton, R. E., 1972, "The response of a turbulent boundary layer to a step change in surface roughness, Part 2: rough to smooth", *Journal of Fluid Mechanics*, Vol. 53, 737-757.

Avelino, M. R., 2000, "An Experimental/Numerical study of the turbulent boundary layer development along a surface with a sudden change in roughness", *Journal of Brazilian Society of Mechanical Sciences*, Vol. 22, No. 1, 93-104.

Balachandar, R., and Ramachandran, S., 1999, "Turbulent boundary layers in low Reynolds number shallow open channel flows", *Trans. ASME Journal of Fluids Engineering*, Vol. 121, No. 3, 684-689.

Balachandar, R., and Patel, V. C., 2002, "Rough wall boundary layer on plates in open Channels", *Journal of Hydraulic Engineering*, Vol. 10, 947-951.

Cui, J., Patel, V. C., and Lin, C-L., 2003, "Large-eddy simulation of turbulent flow in a channel with rib roughness", *International Journal of Heat and Fluid Flow*, Vol. 24, 372-388.

Gad-el-Hak, M., and Bandyopadhyay, P. R., 1994, "Reynolds number effects in wall-bounded turbulent flows", *Applied Mechanics Review*, Vol. 47, No. 8, 307-365.

Grass, A. J., Stuart, R. J., and Mansour-Tehrani, M., 1993, "Common vortical structure of turbulent flows over smooth and rough boundaries", *AIAA Journal*, Vol. 31, No. 5, 837-847.

Krampa-Morlu, F. N., 2001, "Boundary layer wake interaction in an open channel flow", M.Sc. Thesis, Department of Mechanical Engineering, University of Saskatchewan, Saskatoon, Canada.

Krogstad, P. A., Antonia, R. A., and Browne, L. W. B., 1992, "Comparison between Rough- and Smooth-Wall Turbulent Boundary Layers", *Journal of Fluid Mechanics*, Vol. 245, 599-617.

Perry A. E., Schofield, W. H., and Joubert, P. N., 1969, "Rough wall turbulent boundary layers", *Journal Fluid Mechanics*, Vol. 37, 382-413.

Raupach, M. R., 1981, "Conditional Statistics of Reynolds Stress in Rough-Wall and Smooth-Wall Turbulent Boundary Layers", *Journal Fluid Mechanics*, Vol. 108, 363-382.

Schwarz, A. C., Plesniak, M. W., and Murthy, S. N. B., 1999, "Turbulent boundary layers subjected to multiple strains", *Trans ASME Journal of Fluids Engineering*, Vol. 121, 526-32.

Tachie, M. F., 2000, "Near-wall flows on smooth and rough surfaces", Ph.D. Thesis, Department of Mechanical Engineering, University of Saskatchewan, Saskatoon, Canada.

Tani, J., 1987, "Turbulent boundary layer development over rough surfaces", *Perspective in Turbulence Studies, Springer*.

Taylor, R. P., Taylor, J. K., Hosni, M. H., and Coleman, H. W., 1993, "Relaxation of the turbulent boundary layer after an abrupt change from rough to smooth wall", *Trans. ASME Journal of Fluids Engineering*, Vol. 115, 379-382.